## CHARACTERISING THE IN-PLANE SEISMIC PERFORMANCE OF INFILL MASONRY

# Kathy Sassun<sup>1</sup>, Timothy J. Sullivan<sup>2</sup>, Paolo Morandi<sup>3</sup> and Donatello Cardone<sup>4</sup>

(Submitted June 2015; Reviewed September 2015; Accepted December 2015)

#### **ABSTRACT**

Masonry infills, commonly found in frame buildings throughout Europe and other parts of the world, have performed poorly in past earthquakes, with infill damage endangering lives, causing disruption and significant monetary losses. To characterize the performance of masonry infills, commonly classified as non-structural elements, an extensive set of experimental test data is collected and examined in this work in order to develop fragility functions for the in-plane performance of masonry infills. The collected data stems from testing conducted in Europe, the Middle East and the United States and includes solid and hollow clay brick or concrete block infills, constructed to be in contact within either reinforced concrete or steel framing. The results indicate that infill masonry can exhibit first signs of damage at drifts as low as 0.2% but may not suffer complete failure until drifts as high as 2.0%. Furthermore, it is shown that masonry fragility changes significantly according to the type of infill masonry. Subsequently, a short discussion is provided to highlight the potential use of the infill fragility information within non-linear analysis models of masonry infill. Finally, repair cost estimates for infills in Italy are computed using costing-manuals and are compared with cost estimates obtained through consultation with a number of Italian building contractors, with examination of both the median and dispersion in repair costs. It is anticipated that the results of this work will be particularly useful for advanced performance-based earthquake engineering assessments of buildings with masonry infill, providing new information on the in-plane fragility, repair costs and nonlinear modelling of masonry infills.

#### INTRODUCTION

In the seismic design of structures, Force-Based Design (FBD) procedures are most commonly adopted by design codes. In New Zealand this is reflected in the two Standards used for the seismic design of reinforced concrete (RC) structures: NZS1170.5 [1]-Structural Design Actions Part 5: Earthquake Actions and NZS3101-Concrete Structures Standard [2]. It is now known that most code FBD approaches are based on a number of flawed concepts as explained by Priestley [1993, 2003] and these flaws can potentially lead to un-conservative designs. As a result, Displacement-Based Design (DBD) procedures have been developed to correct these issues. The development of DBD procedures is further motivated by the increasing focus on Performance-Based Earthquake Engineering, in which more robust performance levels are established in comparison to the traditional prescriptive approaches and design solutions are tailored to meet client needs. The performance levels are typically based on damage to the structural and non-structural elements, which in turn are directly related to displacements and deformations (or to floor accelerations in the case of acceleration sensitive nonstructural elements and contents). The seismic performance of infilled masonry buildings, such as those shown in Figures 1 and 2, has been poor in past earthquakes, including recent events in Italy such as the 2009 L'Aquila earthquake (see, for example, Ricci et al. [3]) and the 2012 Emilia earthquake (see, for example, Manzini and Morandi [4]).

Nevertheless, analytical studies have also pointed out that the performance of infills and masonry infilled buildings does depend on a number of factors, including the infill typology, aspect ratio and distribution (see, for example, [5], [6], [7]).

A large amount of research has been undertaken to better understand and characterise the behaviour of clay and concrete masonry infilled frame structures (see [7], [8], [9], [10], [11]). Such research has led to a better understanding of the behaviour of the masonry infills, providing insight to the large range of possible failure mechanisms that can develop and enabling the definition of different damage states that will be described in the next section. Masonry panels are commonly constructed in complete contact with the surrounding RC or steel frame without the provision of any gaps or connections around the boundaries; following this construction technique, and noting that the infills are placed only after the surrounding RC frames have hardened, the infills are assumed as non-load bearing such that in European design practice the masonry infills are commonly treated as non-structural elements. Furthermore, even though the elements are deemed nonstructural, damage to masonry infills can represent a threat to life (due to falling mass or hampering safe evacuation of a building) and lead to significant loss of time and money in order to repair the infills and elements affected by damage to infills (such as electrical wiring and windows).

Traditionally, seismic assessment of a building has aimed to check whether prescribed performance limit states for structural elements would be exceeded in certain intensity levels associated with certain probabilities of exceedance. For example, one assessment objective might be to evaluate whether the ductility capacity of a frame structure is exceeded for a 475 year return intensity level. However, modern assessment methodologies, such as the PEER performance-based earthquake engineering (PBEE) approach (FEMA P-58 [12]), are now able to quantify performance parameters such

<sup>&</sup>lt;sup>1</sup> Rose Programme, UME School, IUSS Pavia, Italy, <u>kathysassun@hotmail.com</u>

<sup>&</sup>lt;sup>2</sup> Assistant Professor, University of Pavia and EUCENTRE, Pavia, Italy, <u>timothy.sullivan@canterbury.ac.nz</u> (Member)

<sup>&</sup>lt;sup>3</sup> Researcher, University of Pavia and EUCENTRE, Pavia, Italy

<sup>&</sup>lt;sup>4</sup> Associate Professor, University of Basilicata, Potenza, Italy

as expected monetary losses (for repairs), downtime and injuries, with better consideration of uncertainties in demand and capacity. The PEER PBEE assessment procedure foresees a four stage analysis process; (i) probabilistic seismic hazard assessment to provide information on the probability of certain intensity levels, (ii) structural analysis to establish the likely demands (referred to as engineering demand parameters, EDPs), for a certain intensity level, on structural and non-structural elements, (iii) damage analysis to quantify the likelihood of a component being in a certain damage state given a certain EDP, and (iv) computation of decision variables using consequence functions that provide, for example, the expected monetary loss for a given damage state. For a detailed description of the procedure, see FEMA P-58 [12] or Porter [13].



Figure 1: Infill masonry damage observed following the 2009 L'Aquila Earthquake [3].



Figure 2: Infill masonry in-plane damage observed following the 2012 Emilia Earthquake [4].

In order to facilitate the application of the PEER PBEE procedure to masonry infilled frame buildings typical of Italian construction practice, the objectives of this paper are the following:

- Develop fragility functions for the in-plane response of masonry infills, using existing experimental data, so that the likely damage to a masonry infill can be established for a certain engineering demand parameter (i.e. useful for the damage analysis phase of the PBEE procedure).
- Provide guidance to allow the correlation of non-linear analysis models for masonry infill to the observed fragility information, so that the representation of the masonry infill adopted during the structural analysis phase is

- consistent with the behaviour assumed in the damage analysis phase (i.e. useful for the structural analysis phase of the PBEE procedure).
- Develop cost functions to permit simple quantification of the repair cost that can be expected when the infill masonry is pushed to a certain damage state (i.e. useful for the estimation of monetary loss during the decision variable analysis stage of the PBEE procedure).

The focus will be on the in-plane response of solid and hollow clay brick or concrete block masonry infill, constructed to be in contact within either reinforced concrete or steel framing, and representative of construction practices in Europe, the Middle East and parts of the United States. All of the objectives described above rely on a clear definition of masonry infill damage states. Given that there does not appear to be universal agreement as to the appropriate means of defining damage states in masonry infills, the next section discusses different possible definitions and subsequently clarifies the damage state definitions adopted in this work.

### POSSIBLE DAMAGE STATES FOR INFILL MASONRY

The performance associated with the in-plane response of masonry infills should be evaluated through interpretation of attained levels of damage in the panels. However, a commonly accepted definition of possible damage limit states specifically related to performance requirements for masonry infills has not yet been established within the scientific community and relevant specifications included in international seismic standards and codes are rather inaccurate. Results from a few experimental investigations in the past have provided different definitions of performance limits states applied to masonry infills. For example, Mehrabi and Shing, [14] have proposed 12 Limit States for the description of major events occurring during in-plane tests on infilled RC frames (I: first major crack in infill and sliding; II: maximum lateral load; III: reduction to 80% of maximum lateral load; IV: major crack in column; V: shear crack in beam-column joints; VI: sliding of mortar joints; VII: interior crushing of infill; VIII: corner crushing of infill; IX: yielding of reinforcement in column; X: yielding of reinforcement in beam; XI: crushing of concrete in columns; XII: maximum lateral displacement imposed on specimen). Calvi and Bolognini [10] have assumed four limit states with levels of damage associated to precise points on the forcedisplacement envelope resulting from in-plane cyclic static tests ("LS1": no damage/fully operational, "LS2": light damage/operational, "LS3": severe safety/repairable, "LS4": very heavy damage/life danger). More recently, Hak et al. [15] have considered three performance criteria defined in terms of increasing levels of damage observed during similar in-plane experiments: an "Operational limit state" where the infills are considered undamaged, a "Damage Limitation limit state" where infills are damaged but can be easily and economically repaired and a "Life Safety limit state" where infills are severely damaged and reparability is economically questionable, but lives are not threatened. The definition of different performance levels referring to the state of damage in structural and non-structural components (including infills) is commonly also included in international seismic codes and standards, both for the design of new buildings and for the assessment of existing buildings. Nevertheless, explicit descriptions related to infills are most frequently not available. A general definition of the compliance criteria included in the Italian, European and U.S. seismic codes is briefly reported in the following paragraphs.

### **Definition of Performance Levels for Infills According to International Seismic Codes**

In the European code [16], given definitions of limit states (i.e., Eurocode 8 – Part 1 and Part 3) for the design/assessment of buildings do not comprehensively refer to conditions specifically related to infill damage, and in particular, no explicit criteria are provided to allow a quantification of the acceptable extent of damage. Currently, for the design of new structures, Eurocode 8 – Part 1 refers to a damage limitation and to an ultimate limit state. Referring to fundamental requirements which need to be satisfied, each with an adequate degree of reliability, the code states that at the damage limit state (DLS) the occurrence of damage and the associated limitations of use, the costs of which would be disproportionately high in comparison with the costs of the structure itself, should be prevented, while at the ultimate limit state (ULS) or Life Safety limit state (LSLS) the structure should remain without global or local collapse, thus retaining its structural integrity and a residual load bearing capacity. Related to the corresponding compliance criteria, at the damage limit state an adequate degree of reliability against unacceptable damage shall be ensured by satisfying the deformation limits and at the ultimate limit state it shall be verified that the behaviour of non-structural elements does not present risks to persons and does not have a detrimental effect on the response of structural elements. In the Italian Norms for Construction [17], the conditions corresponding to an operational and a near collapse limit state (this latter being in line with the one included in Eurocode 8 - Part 3 for the assessment of existing structures) are also included; for the operational limit state (OLS) the structure as a whole, including structural and non-structural elements, and equipment relevant to its function, must not be damaged or exposed to any significant disruption of use, whereas for the near collapse limit state (NCLS) the structure may suffer serious damage and collapse of non-structural components and installations as well as serious damage of structural components.

In the U.S. context, according to FEMA E-74 [18], the failure of non-structural components during an earthquake, including partitions and infills, may result in injuries or fatalities, and cause costly property damage to buildings and their contents. Accordingly, the potential consequences of earthquake damage to non-structural components are divided into three types of risk: Life Safety limit state (LS), the limit state after which damage to non-structural elements presents risks to persons, Property Loss limit state (PL), the state after which non-structural damage will imply monetary losses (of property) and a Functional Loss limit state (FL), after which any damage to components will cause interruption to the use of the building. In FEMA 273 [19] three different performance criteria applied for structural components and unreinforced masonry infill walls are included: Immediate Occupancy (S-1), Life Safety (S-3) and Collapse Prevention (S-5), whose definitions roughly correspond, respectively, to the OLS, LSLS and NCLS conditions reported in the European standards. Specifically referring to the performance of masonry infills, FEMA 273 classifies as Immediate Occupancy the situation where minor cracking of masonry infills and veneers and minor spalling in veneers at a few corner openings occurs; as Life Safety the case where extensive cracking and some crushing and spalling of veneers at corners of openings occurs but the walls remain in place without falling units, and, finally, as Collapse Prevention the case where extensive cracking and crushing are present in the infills and some walls dislodge.

### **Definition of Performance Levels for Infills According to In-Plane Cyclic Tests**

Based on the general requirements provided by international standards, a definition of specific performance levels suitable for non-structural masonry infills is adopted within the scope of this study. The limit state definition relies on the performance of a single masonry infill evaluated from the results of in-plane cyclic tests on RC and steel frames. Hence, in line with the objectives of this study, four limit states, specifically referring to masonry infills are here introduced, based on the increasing extent of infill damage:

- Damage State 1 (DS1): "Operational limit state". The infill is considered slightly damaged. The occurrence of this level of damage, usually subsequent to the detachment of the masonry panel from the RC frame at the intrados of the top beam and along the (upper) height of the columns, can be characterized by a very light and superficial cracking in the masonry panel, mainly concentrated in the bed- and in the head-joints, or by cracks in the plaster. A "Cosmetic" damage without the need for repair, like very light cracks in the plaster, does not belong to this damage state and it is not considered here.
- Damage State 2 (DS2): "Damage Limitation limit state". The infill is damaged, but can be effectively and economically repaired. Damage of the infill panel, through the formation of bi-diagonal cracking, involving both the joints and the units or diagonal step-wise cracking affecting mainly the bed and the head-joints, is expected to occur. Sliding in the bed-joints may also occur. Very limited crushing and spalling of a few units, for instance at the upper corners and/or at the top edge of the infill, can be assumed to occur.
- Damage State 3 (DS3): "Life Safety or Significant Damage limit state". The infill is severely damaged and reparability is economically questionable, however, lives are not threatened. Detachment of large plaster area, significant sliding in the mortar joints and further development of cracks in the units can be expected to occur. In addition, crushing and spalling of brick units are more widespread on the panel. The wall is not repairable at reasonable costs (it is more convenient to demolish and reconstruct the entire wall), however the position and the weight of masonry portions falling down is so limited as to exclude the risk for the loss of human lives. In case of openings in the infill, the window is considered not damaged, however it has to be removed and installed again in order to allow the repair of the infill itself.
- Damage State 4 (DS4): "Near Collapse limit state". The infill is close to collapse. A large amount masonry panel area is assumed to be affected by crushing/spalling of blocks/bricks and the panel is close to collapse. In case of openings in the infill, the window is considered damaged and it has to be replaced by a new one.

With reference to the definition provided above, the performance levels for a single masonry infill unit have been identified in terms of inter-storey drift ( $\theta$ ) associated with a specific degree of damage derived from available results of inplane cyclic tests on infilled frames, computing the drift  $\theta$  as the ratio between the horizontal displacement and the height at the beam centreline of the specimen. Therefore, for each experimental test on a particular type of infill, a value of drift corresponding to the attainment of a specific Damage State is to be selected based on the extent of infill damage determined following the interpretation of existing documentation (such as journal publications or test reports), including pictures of test specimens and the description of observations documented

Table 1: Comparison of performance levels for slender weak (Calvi and Bolognini, [10] revised by Hak et al., [15]) and strong masonry infills (Morandi et al., [8]). For the slender infill the test was stopped before attaining a near collapse situation.

	Slender infill	Strong infill
DS1	drift $\theta \sim 0.20 \%$	drift $\theta$ =0.30 %
DS2	drift θ ~ 0.30 %	drift $\theta$ =0.50 %
DS3	drift θ ~ 1.00 %	drift $\theta$ =1.75 %
DS4	(slender infill not pushed to DS4)	drift θ=2.50 %

during the tests which have been taken into consideration. An example of drift limits obtained for the four Damage States is reported in Table 1, for the case of a weak infill (horizontally hollowed 115 mm thick clay units with plaster, Calvi and Bolognini, [10] revised by Hak et al., [15]) and a strong infill (vertically hollowed 350 mm thick clay units without plaster, Morandi et al., [8]).

Such interpretation of in-plane cyclic tests, accounting primarily for the correlation of damage levels and values of drift, could sometimes result in biased and subjective conclusions, in particular, given the aim of providing a qualitative definition of the damage states. A possible solution to this issue could be the association of damage levels with specific points on the experimental force-displacement curve. Based on the experimental results of in-plane cyclic tests, such a simplified procedure consists in the evaluation of the average response of the masonry infill estimated as the difference between the average experimental envelope of the infilled frame and the average experimental envelope of the corresponding bare frame configuration, as reported in more detail in Hak et al., [15]. On the determined response curve, characterizing the infill contribution to the lateral response of the infilled frame, points representing the attainment of some of the defined Damage States could be identified; for example, DS2 could be as assigned to the peak of the envelope or to the beginning of a possible strength plateau, as commonly assumed for load-bearing masonry walls when first large cracking affecting units and joints occurs and a damage limitation state is attained (see e.g., Morandi et al., [8]); moreover, DS3 and DS4 could correspond to different postpeak strength degradation ratios. Nevertheless, this approach appears to be rather conventional and significantly dependent on the considered masonry infill typology, particularly for what regards the definition of the strength reduction corresponding to limit states DS3 and DS4; hence, for the needs of this study, force-displacement considerations have only been applied to check the validity of the results obtained by visual interpretation of damage assigned to damage level DS2, relying on tests for which sufficient and reliable experimental data were available.

### DEVELOPMENT OF FRAGILITY FUNCTIONS FOR INFILL MASONRY

In earthquake engineering, a fragility curve is a statistical cumulative distribution function that provides the probability of developing a certain damage state given a value of engineering demand. As explained earlier, fragility functions are used in the damage analysis phase of the PEER PBEE assessment procedure, relating the results of structural analyses (providing engineering demand parameters) to damage states. In this section, the results of experimental data reported in the literature are used to propose fragility curves for masonry infill walls.

#### $\label{lem:collection} \textbf{Collection of Experimental Data from the Literature}$

As mentioned in the introduction, a large amount of experimental data is available in the literature. However, as discussed in the previous section, interpreting the boundaries of different damage states from experimental results is not straight-forward for infill masonry, and in this work efforts have been made to ensure that the physically observed damage is used to identify the onset of a damage state, rather than make reference to a force-displacement response. As such, the experimental data utilized in this work considers data from publications where visual descriptions of the damage and relative drifts were reported and where the non-structural masonry infill was not scaled significantly in size. Table 2 summarizes the specimens analysed (type of masonry unit,

type of mortar, infill thickness), while Table 3 reports the drift at the attainment of different damaged states, also described in the table, as assessed from the experimental data. With the exception of the infill tested by Calvi and Bolognini [10], all the other masonry panels were realized without plaster. As such, it was not possible to study the influence, which may be significant, of plaster on the in-plane response of masonry infills and this should be an area for future research. The different damage states related to the masonry infill walls were defined and associated considering the repair efforts needed to restore that wall to an undamaged state. This is considered particularly important considering that the fragility functions obtained from this data should be used together with relevant repair cost (consequence) functions provided later in this paper.

#### **Storey Drift-Based Fragility Functions**

In developing a fragility function, it is useful to choose a common form for the probability density function (PDF), such as a normal distribution or a log-normal distribution. While various distributions may be able to represent the data well, the lognormal distribution is commonly used when the values of the random variable are known to be strictly positive, as in engineering. As such, the fragility functions developed in this work for masonry infill are assumed to follow a log-normal distribution, such that the conditional probability,  $F_i(EDP)$  that the infill will be damaged to damage state "i", as a function of engineering demand parameter (EDP), is given by:

$$F_{i}(EDP) = \Phi\left(\frac{\ln(EDP/\bar{x}_{i})}{\beta_{i}}\right)$$
 (1)

where  $\Phi$  denotes the standard normal (Gaussian) cumulative distribution function,  $\bar{x}_i$  denotes the median value of the probability distribution and  $\beta_i$  denotes the logarithmic standard deviation.

From Eq.(1) it is apparent that a log-normal fragility function can be completely described by the median value and the dispersion of the function. In this work, the median and dispersion for the drift capacity at each damage state was computed directly from the experimental results reported in Table 3 (using the approach that Porter *et al.* [20] refer to as Method A; Actual EDP). Figure 3 and Tables 4-5 present the results obtained for the whole dataset, compared with the sorted experimental data. Note that the Lilliefors goodness of fit test [21] was used to check the quality of the resulting lognormal distributions (using Pierce's criterion for identification of outliers) and in all cases the lognormal distribution was seen to satisfy a 5% significance level.

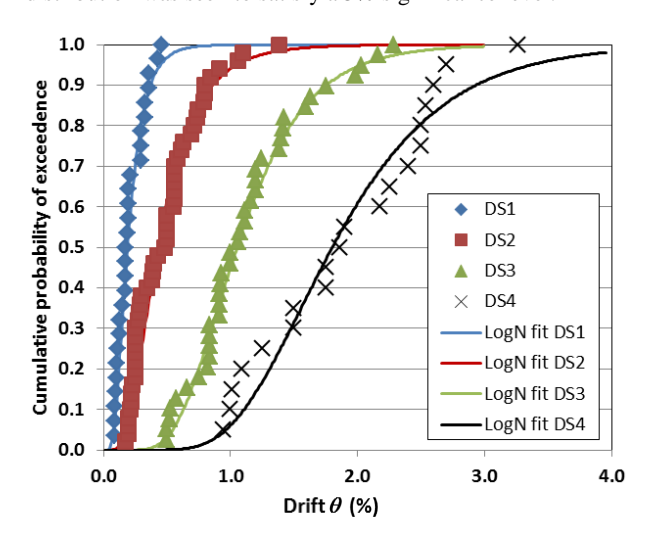


Figure 3: Cumulative density functions for drift.

Table 2: Masonry infill wall characteristics.

REF	Test label	Masonry unit	Description of masonry unit	Mortar type compression strength	Wall thickness
[6]	2a 3a		Brick thickness: 46 mm	Type N (8.3 MPa) Lime Mortar (6.2 MPa)	46 mm
Scale 2:3	6a	Solid clay brick	D. I. I. I	Lime Mortar (6.2 MPa)	92 mm
RC frame	7a 8a		Brick thickness: 92 mm	Type N (8.3 MPa) Lime Mortar (6.2 MPa)	194 mm
	3	Solid concrete block		Emile Mortal (0.2 mil a)	17111111
	4	Hollow concrete block			
	5 6	Solid concrete block Hollow concrete block			
[14]	7	Solid concrete block	Unit dimensions (txlxh): 100x200x100 mm	15 MD	100
Scale 1:2 RC frame	8	Hollow concrete block	Hollow concrete block: vertical holes approx. 50%	~15 MPa	100 mm
110 1141110	9	Solid concrete block Hollow concrete block	approxit 50%		
	11	Solid concrete block			
	12	Solid concrete block			
[30]	S2-N -II (2 bays)		Unit dimensions (txlxh): 50x50x100 mm	14.8 MPa	
Scale 1:4 Steel frame	S2-SYM (2 bays) S2-ASYM	Hollow concrete block	Hollow concrete block: vertical holes approx. 50%	11.7 MPa	50 mm
Tranic	(2 bays)			21.4 MPa	
[28]	40W1				400 mm
Scale 2:3	40W2 60W1	Solid clay brick	Brick dimensions (txlxh): 100x200x50 mm	Type N (min. 6.2 MPa)	400 mm 600 mm
Steel	60W2	Solid clay blick	Dick difficusions (talan). 100x200x30 film	Type IV (IIIII. 0.2 IVII a)	600 mm
frame	80W1				800 mm
	C1 C2		U. 4 dimension (4-1-1), 120-250-120		120 mm 120 mm
[7]	L1		Unit dimension (txlxh): 120x250x120 mm Vertical holes approx. 53%	Cement-lime (5 and	120 mm
Scale 1:2 RC frame	L2	Hollow clay unit		10 MPa)	120 mm
KC Iraine	N1 N2		Unit dimension (txlxh): 80x250x120 Horizontal holes approx. 53%		80 mm 80 mm
[10] -[15] Scale 1:1 RC frame	2	Hollow clay unit	Unit dimension (txlxh): 115x245x245 mm Horizontal holes 60%	Cement-Lime (5.5 MPa)	115mm
[22] Scale 3:4 RC frame	Unit 1	Solid concrete block	Unit dimension (txlxh): 90x230x75 mm	Cement-lime (8.0 MPa)	90 mm
[33] Scale 3:4 RC frame	-	Clay brick	Brick dimension (txlxh): 102x203x68mm Vertical holes	Type N (min. 6.2 MPa)	102 mm
[11] Scale 1:3 RC frame	S WO2 DO2	Hollow clay unit	Unit dimension (txlxh): 60x93x60 mm Horizontal holes	M1 (1.53 MPa)	60 mm
[32] Scale 1:1 RC frame	-	Solid clay brick	Brick dimension (txlxh): 92x194x57 mm	Type N (10 MPa)	92 mm
[9] Scale 2:3 Steel frame	SW PW1 PW2 PW3 PW4	Solid clay brick	Brick dimension (txlxh): 110x219x66mm	Cement (10.1 MPa)	110 mm
[31] Scale 1:1 RC frame	URM_V	Hollow clay unit	Unit dimension (txlxh): 300x240x195mm Vertical holes 50%	M10 (19.9 MPa)	300 mm
[29] Scale 1:2.5 RC frame	III/2 I/1 I/2 I/3 I/4	Hollow clay brick	Unit dimension (txlxh): 120x250x95 mm Vertical holes approx. <55%	Cement-lime M5 (5.2 MPa)	120 mm
[8] Scale 1.1 RC frame	TA1 TA2 TA3	Hollow clay unit	Unit dimension (txlxh): 350x235x235 mm Vertical holes 50%	M5 (7.7 MPa)	350 mm

Table 3: Literature review of masonry infill wall damage and DSs.

REF	Test label	L (m)	H (m)	L/H	Openings	Limit State	Damage description	θ (%)	ε (-)
		2.74	1.78	1.54		DS1	Initial cracks and beginning of separation of the infill from the panel	0.17%	0.0008
	2a	2.74	1.78	1.54		DS2	Development of diagonal cracks in the centre of the infill wall	0.34%	0.0016
	3a	2.74	1.78	1.54		DS1	Initial cracks and beginning of separation of the infill from the panel	0.11%	0.0005
		2.74	1.78	1.54		DS2	Extension of the previous cracks	0.22%	0.0010
[6] Scale 2:3	6a	2.74	1.78	1.54	w/o	DS1	Initial cracks and beginning of separation of the infill from the panel	0.13%	0.0006
RC frame		2.74	1.78	1.54	-	DS2	Extension of the previous cracks	0.25%	0.0011
	7a	2.74	1.78	1.54		DS1	Initial cracks and beginning of separation of the infill from the panel	0.13%	0.0006
		2.74	1.78	1.54		DS2	Extension of the previous cracks	0.25%	0.0011
	8a	2.74	1.78	1.54		DS1	Initial cracks and beginning of separation of the infill from the panel	0.20%	0.0009
		2.74	1.78	1.54		DS2	Development of diagonal cracks in the centre of the infill wall	0.39%	0.0018
		2.31	1.54	1.50		DS1	First cracks in the infill wall	0.21%	0.0010
	3	2.31	1.54	1.50		DS2	Maximum resistance	0.21%	0.0010
		2.31	1.54	1.50		DS3	Internal wall crushing	1.16%	0.0053
	4	2.31	1.54	1.50		DS1	First cracks in the infill wall	0.17%	0.0008
		2.31	1.54	1.50		DS2	Maximum resistance	0.63%	0.0029
		2.31	1.54	1.50		DS3	Internal wall crushing	1.24%	0.0057
		2.31	1.54	1.50		DS1	First cracks in the infill wall	0.33%	0.0015
	5	2.31	1.54	1.50		DS2	Maximum resistance	0.79%	0.0036
		2.31	1.54	1.50		DS3	Internal wall crushing	1.40%	0.0064
		2.31	1.54	1.50		DS1	First cracks in the infill wall	0.36%	0.0017
	6	2.31	1.54	1.50		DS2	Maximum resistance	0.61%	0.0028
		2.31	1.54	1.50		DS3	Internal wall crushing	0.91%	0.0042
		2.31	1.54	1.50		DS1	First cracks in the infill wall	0.46%	0.0021
	7	2.31	1.54	1.50		DS2	Maximum resistance	0.71%	0.0033
[14] Scale 1:2		2.31	1.54	1.50	w/o	DS3	Corner wall crushing	0.82%	0.0038
RC frame		2.31	1.54	1.50	W/O	DS1	First cracks in the infill wall	0.20%	0.0009
	8	2.31	1.54	1.50		DS2	Maximum resistance	0.91%	0.0042
		2.31	1.54	1.50		DS3	Internal wall crushing	1.59%	0.0073
		2.31	1.54	1.50		DS1	First cracks in the infill wall	0.33%	0.0015
	9	2.31	1.54	1.50		DS2	Maximum resistance	0.48%	0.0022
		2.31	1.54	1.50		DS3	80% of maximum resistance	1.98%	0.0091
		3.12	1.54	2.03		DS1	First cracks in the infill wall	0.17%	0.0007
	10	3.12	1.54	2.03		DS2	Maximum resistance	0.40%	0.0016
		3.12	1.54	2.03	]	DS3	Corner wall crushing	0.91%	0.0036
		3.12	1.54	2.03	]	DS1	First cracks in the infill wall	0.36%	0.0014
	11	3.12	1.54	2.03	]	DS2	Maximum resistance	0.74%	0.0029
		3.12	1.54	2.03	]	DS3	Internal wall crushing	0.91%	0.0036
	_	3.12	1.54	2.03	]	DS1	First cracks in the infill wall	0.17%	0.0007
	12	3.12	1.54	2.03	]	DS2	Maximum resistance	0.55%	0.0022
		3.12	1.54	2.03		DS3	Internal wall crushing	0.66%	0.0026

Table 3 (continued): Literature review of masonry infill wall damage and DSs.

REF	Test label	L (m)	H (m)	L/H	Openings	Limit State	Damage description	θ (%)	ε (-)
	S2-N-II	1.80	0.94	1.92	w/o	DS2	Horizontal cracks at the centre of the infill	0.69%	0.0028
	(2 bays)	1.80	0.94	1.92	w/o	DS4	Mortar cracking	1.86%	0.0076
[30]	S2-SYM	1.80	0.94	1.92	1 window 1door	DS2	Initial cracks at the corner of openings	0.80%	0.0033
Scale 1:4 Steel frame	(2 bays)	1.80	0.94	1.92	2 windows 1door	DS4	Several cracks along the mortar bed and head joints	2.54%	0.0104
	S2-ASYM	1.80	0.94	1.92	2 windows	DS2	Initial cracks at the corner of openings	0.58%	0.0024
	(2 bays)	1.80	0.94	1.92	2 windows	DS4	Several cracks along the mortar bed and head joints	3.26%	0.0133
		1.75	1.65	1.06		DS2	Cracks in the bed joints	0.25%	0.00125
	40W1	1.75	1.65	1.06		DS3	Cracks formed in the head joint	0.75%	0.00374
		1.75	1.65	1.06	]	DS4	Failure of the infill wall	1.25%	0.00622
		1.75	1.65	1.06		DS2	Cracks in the bed joints	0.25%	0.00125
	40W2	1.75	1.65	1.06		DS3	Cracks formed at both brick-mortar interfaces in the bed-joint and on head-joint sometimes	1.38%	0.00687
		1.75	1.65	1.06		DS4	Failure of the infill wall	2.25%	0.01117
		1.75	1.65	1.06		DS2	Cracks in the bed joints	0.25%	0.00125
[28] Scale 2:3 Steel frame	60W1	1.75	1.65	1.06	window	DS3	Vertical cracking in the brick and some flaking of the surface of the brick	1.07%	0.00533
		1.75	1.65	1.06		DS4	Failure of the infill wall	1.50%	0.00746
		1.75	1.65	1.06		DS2	Cracks in the bed joints	0.25%	0.00125
	60W2	1.75	1.65	1.06		DS3	Diagonal compression splitting was clearly apparent. which was a combination of mortar and brick cracking	1.20%	0.00597
		1.75	1.65	1.06		DS4	Failure of the infill wall	1.75%	0.00870
	90W1	1.75	1.65	1.06		DS2	Cracks formed through the head joints and the brick.	0.25%	0.00125
	80W1	1.75	1.65	1.06		DS3	Diagonal compression splitting became more pronounced	0.93%	0.00463
	C1	1.90	1.43	1.33		DS2	Significant cracks, with some bricks showing tensile splitting of their ribs	0.43%	0.00206
		1.90	1.43	1.33		DS3	Crush in the centre of the infill wall	1.42%	0.00680
	C2	1.90	1.43	1.33	-	DS2	Significant cracks, with some bricks showing tensile splitting of their ribs	1.06%	0.00508
		1.90	1.43	1.33		DS3	Crush in the centre of the infill wall	1.06%	0.00508
	L1	2.50	1.43	1.75		DS2	Significant cracks, with some bricks showing tensile splitting of their ribs	1.38%	0.00593
[ <b>7</b> ] Scale 1:2	LI	2.50	1.43	1.75	w/o	DS3	Crush at the corners of the infill wall	1.63%	0.00700
RC frame	L2	2.50	1.43	1.75		DS2	Significant cracks, with some bricks showing tensile splitting of their ribs	1.10%	0.00473
		2.50	1.43	1.75		DS3	Crush at the corners of the infill wall	2.28%	0.00979
	271	2.50	1.43	1.75	=	DS2	Some horizontal sliding at mid-height	0.80%	0.00344
	N1	2.50	1.43	1.75	]	DS3	Crush at the corners of the infill wall	2.03%	0.00872
		2.50	1.43	1.75	1	DS2	Some horizontal sliding at mid-height	0.84%	0.00361
	N2	2.50	1.43	1.75	1	DS3	Crush at the corners of the infill wall	2.16%	0.00928
		4.50	2.88	1.57		DS1	Cracks in the plaster	0.19%	0.0009
[10] -[15]	2	4.50	2.88	1.57	w/o	DS2	Diagonal cracks in the masonry	0.29%	0.0013
Scale 1:1 RC frame		4.50	2.88	1.57		DS3	Crushing and spalling of units	0.99%	0.0045

Table 3 (continued): Literature review of masonry infill wall damage and DSs.

REF	Test label	L (m)	H (m)	L/H	Openings	Limit State	Damage description	θ (%)	ε (-)
[22]		2.667	2.10	1.27		DS1	Small cracks in the upper part of the masonry panel	0.20%	0.0010
Scale 3:4	Unit 1	2.667	2.10	1.27	w/o	DS2	Start of sliding along the shear cracks	0.30%	0.0015
RC frame		2.667	2.10	1.27		DS4	Severe cracking of the panel, sliding failure	1.50%	0.0073
		4.11	2.75	1.49		DS1	First significant sign of damage: some small vertical splitting cracks are observed in the mortar head joints at the URM infill wall corners	0.43%	0.0018
[ <b>33</b> ] Scale 3:4		4.11	2.75	1.49	,	DS2	Significant URM infill wall cracks with clear pattern and load path definitions are formed	0.74%	0.0032
RC frame Shaking table	-	4.11	2.75	1.49	w/o	DS3	Further damage in the URM infill wall: a major horizontal (along bed joint) crack in the URM infill wall is developed at about one third of the infill wall height from the bottom	1.41%	0.0061
		4.11	2.75	1.49		DS4	Gradual global disintegration of the URM infill wall	2.17%	0.0094
	S	1.35	0.90	1.50	w/o	DS2	First cracks in the infill wall	0.28%	0.0013
	S	1.35	0.90	1.50	W/O	DS3	DS3 Sliding along bed joints		0.0042
[11] Scale 1:3	WO	1.35	0.90	1.50		DS2	First cracks in the infill wall	0.38%	0.0018
RC frame	WO2	1.35	0.90	1.50	window	DS3	Diagonal cracks	1.11%	0.0051
	D02	1.35	0.90	1.50		DS2	First cracks in the infill wall	0.27%	0.0012
	DO2 1.35 0.90		0.90	1.50	door	DS3	Shear sliding	1.20%	0.0055
		6.10	3.05	2.00		DS1	First cracks in the infill wall	0.15%	0.00060
[32]		6.10	3.05	2.00	]	DS2	Wider cracks plus additional big cracks	0.20%	0.00080
Scale 1:1	2 bays, 1 infilled,	6.10	3.05	2.00	/-	DS3	Very wide cracks in the infill (max crack width: 9.5 mm)	1.00%	0.00400
RC frame Shaking table	3 storeys	6.10	3.05	2.00	. w/o	DS4	The walls showed perceptible distortion, large holes near mid-height and at lower corners and uppermost layer of brick had disintegrated	1.75%	0.00699
		2.40	1.87	1.28		DS2	Cracks in the infill wall	0.56%	0.0026
	SW	2.40	1.87	1.28	w/o	DS3	Two off-diagonal cracks were formed in the panel along the compression diagonal	1.11%	0.0052
		2.40	1.87	1.28		DS4	Excessive deflection of the infill	2.70%	0.0130
		2.40	1.87	1.28		DS2	Cracks in the infill wall	0.56%	0.0026
	PW1	2.40	1.87	1.28		DS3	Corner crushing of the infill, bricks spalling along the compression strut	0.83%	0.0039
		2.40	1.87	1.28		DS4	Excessive deflection of the infill	2.40%	0.0116
[9]		2.40	1.87	1.28		DS2	Inclined cracks in the infill wall	0.56%	0.0026
Scale 2:3 Steel frame	PW2	2.40	1.87	1.28	window	DS3	Corner crushing of the infill, bricks spalling along the compression strut	0.83%	0.0039
		2.40	1.87	1.28		DS4	Excessive deflection of the infill	1.90%	0.0092
	DIVIC	2.40	1.87	1.28		DS2	Cracks in the infill wall	0.56%	0.0026
	PW3	2.40	1.87	1.28		DS3	Crushing of the infill top of the left pier	0.83%	0.0039
		2.40	1.87	1.28		DS4	Excessive deflection of the infill	2.60%	0.0126
	PW4	2.40	1.87	1.28	door	DS2 DS3	Flexural cracks  Crushing of the side pier, bringing	0.56%	0.0026
		2.40	1.87	1.28	<del> </del>	DS4	deterioration to the infill  Excessive deflection of the infill	2.50%	0.0121
<u> </u>		۷.⊤∪	1.07	1.20		シロサ	Excessive deflection of the lilling	2.30/0	0.0121

Table 3 (continued): Literature review of masonry infill wall damage and DSs.

REF	Test label	L (m)	H (m)	L/H	Openings	Limit State	Damage description	θ (%)	ε (-)
[31] Scale 1:1	LIDM V	4.45	2.78	1.60	w/a	DS1	First visible cracks between columns and URM infill wall and very light cracks in the masonry	0.10%	0.00040
RC frame	URM_V	4.45	2.78	1.60	w/o	DS2	Diagonal cracks in the middle of infill wall	0.50%	0.00224
KC frame		4.45	2.78	1.60		DS3	Further diagonal cracks and strong damage in the infill wall	1.20%	0.00538
		2.00	1.40	1.43		DS1	Initial cracks in the infill wall	0.09%	0.00042
		2.00	1.40	1.43		DS2	Sliding and step-wise cracks in the mortar joints	0.20%	0.00094
	III/2	2.00	1.40	1.43	w/o	DS3	Heavy cracking and crushing of the units	0.57%	0.00268
		2.00	1.40	1.43		DS4	Diagonal and horizontal shear failure in the masonry infill; large amount of crushing/spalling of units at the infill- column interface	1.09%	0.00511
		2.00	1.40	1.43		DS1	Initial cracks in the infill wall	0.10%	0.00047
	I/1	2.00	1.40	1.43	door	DS2	Cracks in the mortar joints / diagonal cracks in the units	0.20%	0.00094
		2.00	1.40	1.43		DS3	Diagonal shear failure and crushing of units	0.50%	0.00235
[29]		2.00	1.40	1.43		DS1	Initial cracks in the infill wall	0.09%	0.00042
Scale 1:2.5 RC frame	I/2	2.00	1.40	1.43	window	DS2	Cracks in the mortar joints / diagonal cracks in the units	0.23%	0.00108
		2.00	1.40	1.43		DS3	Diagonal shear failure and crushing of units	0.52%	0.00244
		2.00	1.40	1.43		DS4	Large amount of crushing/spalling of units	1.01%	0.00474
		2.00	1.40	1.43		DS1	Initial cracks in the infill wall	0.09%	0.00042
	I/3	2.00	1.40	1.43	Eccentric door	DS2	Cracks in the mortar joints / diagonal cracks in the units	0.17%	0.00080
	_	2.00	1.40	1.43		DS3	Diagonal shear failure and crushing of units	0.53%	0.00249
		2.00	1.40	1.43		DS4	Large amount of crushing/spalling of units	0.94%	0.00441
		2.00	1.40	1.43		DS1	Initial cracks in the infill wall	0.10%	0.00047
	I/4	2.00	1.40	1.43	Eccentric window	DS2	Cracks in the mortar joints / diagonal cracks in the units	0.22%	0.00103
		2.00	1.40	1.43		DS3	Diagonal shear failure and crushing of units	0.50%	0.00235
		2.00	1.40	1.43		DS4	Large amount of crushing/spalling of units	1.00%	0.00469
		4.57	3.13	1.46		DS1	Pieces of plaster started to detach	0.30%	0.00140
		4.57	3.13	1.46		DS2	Diagonal cracks appeared on units, damaged blocks in the upper left corner started to detach	0.50%	0.00233
	TA1	4.57	3.13	1.46		DS3	Majority of masonry blocks in the top course and several blocks in the lower central part were strongly damaged.	1.75%	0.00814
[8]		4.57	3.13	1.46	vv/o	DS4	The infill was considerably damaged and close to collapse	2.50%	0.01162
Scale 1:1 RC frame		4.57	3.13	1.46	w/o	DS1	Pieces of plaster started to detach	0.30%	0.00140
re nume	TA2	4.57	3.13	1.46		DS2	Diagonal cracks appeared on units, damaged blocks in the upper left corner started to detach	0.50%	0.00233
		4.57	3.13	1.46		DS1	Pieces of plaster started to detach	0.30%	0.00140
	TA3	4.57	3.13	1.46		DS2	Diagonal cracks appeared on units, damaged blocks in the upper left corner started to detach	0.50%	0.00233

Table 4 also reports the median and dispersion in the storey drift capacity for two different types of masonry infill: solid clay brick infills and clay unit infills with vertical holes. From these results it becomes apparent that the infill typology can affect the fragility of masonry infills. As such, it is concluded that whenever possible and practical, the seismic performance assessment of a masonry infill building should consider the masonry infill typology.

#### **Diagonal Strain-Based Fragility Functions**

As an alternative to defining the fragility as a function of the storey drift, this work also investigates the possibility of defining infill fragility as a function of the axial strain in an equivalent single-diagonal strut model. This is done because the equivalent single-diagonal strut model is commonly used for the analytical representation of masonry infills (as

explained further in the next section) and recent work by Hak  $et\ al.\ [15]$  has indicated that the drift capacity can be directly related to the apparent strain capacity of an equivalent diagonal strut,  $\varepsilon$ , and aspect ratio of the infill panel, L/h. This lead Hak  $et\ al.\ [15]$  to propose that the drift capacity of an infill panel  $\theta$ , expressed as a drift ratio (i.e. the lateral displacement of storey  $d_r$  divided by storey height h), can be computed as:

$$\theta = \frac{d_r}{h} = \frac{L}{h} - \sqrt{(1 - \varepsilon)^2 \left[1 + \left(\frac{L}{h}\right)^2\right] - 1}$$
 (2)

where the aspect ratio is defined as the ratio of frame centreline span, L, divided by the frame centreline storey height, h.

Rearranging Eq. (2) in terms of strain, one can compute the apparent strain capacity of the infill panels  $\varepsilon$ , as a function of the panel geometry and observed drift capacity:

$$\varepsilon = 1 - \sqrt{\frac{1 + \left(\frac{L}{h} - \delta\right)^2}{1 + \left(\frac{L}{h}\right)^2}} \tag{3}$$

Using Eq.(3), the apparent strain capacity of an equivalent diagonal strut was computed for each of the test specimens, and the results are reported on the rightmost column of Table 3. Using these results, diagonal strain-based fragility functions are defined, using the same procedure described in the previous subsection and the results are reported in Table 5.

Comparing the results in Table 5 with those of Table 4, it appears that the dispersion is not greatly affected by the consideration of the equivalent diagonal strut concept, which in turn suggests that the relationship between the aspect ratio and the drift capacity may, in fact, be weak. However, the results presented include strain values derived for a wide range of masonry infill types and dimensions. If data were available for a large set of infills possessing the same type of masonry but different aspect ratios, then it is expected that the strain-based approach would yield more accurate results. Furthermore, the strain-based approach is worth considering further as it may be convenient for analyses, directly relating

the masonry infill capacity to the strain in an equivalent diagonal strut, and will be discussed further in the next section.

### CORRELATING NON-LINEAR ANALYSIS MODELS TO THE OBSERVED FRAGILITY INFORMATION

#### **Overview of Different Modelling Strategies**

The correct modelling of masonry infills is a key issue for an accurate evaluation of the seismic performance of existing frame buildings.

Several models have been proposed in the literature to describe the in-plane lateral behaviour of masonry infills. A crude classification can be made distinguishing between the level of complexity of the model (from phenomenological or macro-model to finite element models), and the ability to capture alternative failure mechanisms in the infill panel (e.g. horizontal slip, diagonal cracking, corner crushing), as well as local effects due to the interaction with the surrounding frame reinforced concrete column shear failure). (e.g. Comprehensive reviews of alternative numerical models for masonry infills can be found in Crisafulli et al. [22].

Certainly, the use of axial springs acting as equivalent compression-only diagonal struts currently appears to be the most widely adopted means of modelling the interaction between masonry infills and frames, due to its simplicity and reliability. Equivalent strut models can be further classified according to the number of struts used to simulate the diagonal compressive action of the infill. The simplest option is to use a single equivalent strut (see Fig.4).

This solution, however, is not able to describe accurately local effects due to the masonry interaction with the frame, because of the connection of the strut directly to the beam–column joints. As such, the interaction with the boundary frame can be simulated using multiple (two or three) off-diagonal equivalent struts, which transfer shear forces and bending moments to beams and columns.

Table 4: Median drift capacity and associated values of dispersion obtained using the experimental dataset.

Limit State	All Typologi	es of infills	Solid clay b	rick infills	Clay brick infills with vertical holes		
	Median (%)	Dispersion	Median (%)	Dispersion	Median (%)	Dispersion	
Operational (DS1)	0.18	0.52	0.14	0.36	0.16	0.68	
Damage Limitation (DS2)	0.46	0.54	0.33	0.48	0.44	0.70	
Life Safety (DS3)	1.05	0.40	0.96	0.21	0.97	0.58	
Ultimate (DS4)	1.88	0.38	2.00	0.28	1.33	0.55	

Table 5: Median strain capacity and associated values of dispersion obtained using the experimental dataset together with an equivalent diagonal strut concept.

	All Typologi	es of infills	Solid clay b	rick infills	Clay brick infills with vertical holes		
Limit State	Median ε (x100)	Dispersion	Median ε (x100)	Dispersion	Median ε (x100)	Dispersion	
Operational (DS1)	0.08	0.51	0.06	0.37	0.07	0.67	
Damage Limitation (DS2)	0.22	0.52	0.16	0.48	0.21	0.67	
Life Safety (DS3)	0.51	0.40	0.47	0.20	0.45	0.55	
Ultimate (DS4)	0.89	0.37	0.96	0.30	0.63	0.54	

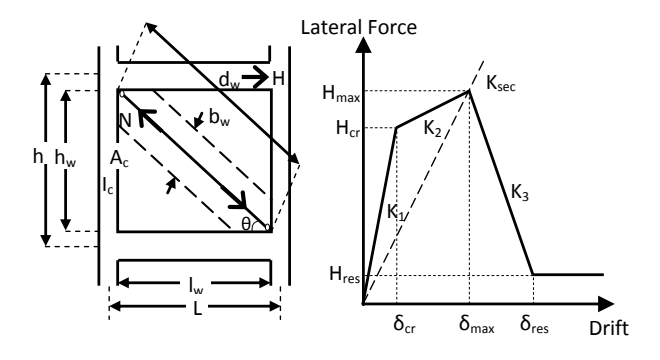


Figure 4: Trilinear lateral force vs. interstorey drift relationship proposed by Panagiotakos and Fardis [23] and Decanini et al. [24] to describe the monotonic behaviour of the equivalent strut model.

Several semi-empirical relationships have been proposed to describe the parameters governing the monotonic and cyclic behaviour of the diagonal strut, as a function of the mechanical and geometrical characteristics of masonry infill. Herein, the attention is focused on the models by Panagiotakos and Fardis [23] and Decanini *et al.* [24].

The model by Panagiotakos and Fardis [23] assumes a threelinear lateral force-displacement skeleton curve, whose corner points represent the cracking force, peak-strength and residual strength after failure of the masonry infill. The model is governed by the following six parameters:

(i) Initial (uncracked) shear stiffness ( $K_1$  in Fig.4), evaluated using the following expression:

$$K_1 = G_m \cdot l_w \cdot t_w / h_w \tag{4}$$

where  $l_w$ ,  $t_w$  and  $h_w$  are the masonry panel length, thickness and height, respectively, and  $G_m$  is the shear modulus of masonry resulting from diagonal compression tests on wallettes;

(ii) Secant stiffness to peak strength ( $K_{sec}$  in Fig. 4), determined from the axial stiffness of the equivalent strut ( $E_m \cdot t_w \cdot b_w/d_w$ ) with width  $b_w$  computed according to the Mainstone formula, as reported in Klinger and Bertero [25]:

$$b_w = 0.175(\lambda h)^{-0.4} \cdot d_w \tag{5}$$

in which  $d_w = \sqrt{l_w^2 + h_w^2}$  is the length of the equivalent strut and  $\lambda h$  is a non-dimensional parameter depending on the geometric and mechanical characteristics of the frame-infill system:

$$\lambda h = \sqrt[4]{\frac{E_m \cdot t_w \cdot sen(2\theta)}{4 \cdot E_c \cdot l_c \cdot h_w}} h \tag{6}$$

where  $E_m$  and  $E_c$  are the Young's moduli of masonry and concrete, respectively,  $\theta$  is the angle between the equivalent strut and the horizontal axis,  $t_w$  and  $h_w$  are the thickness and height of the masonry panel, respectively, h is the storey height and  $I_c$  is the inertia moment of the column cross-section;

- (iii) Softening stiffness ( $K_3$  in Fig. 4), taken equal to 0.5% of the initial stiffness;
- (iv) Lateral cracking strength, assumed equal to:

$$H_{cr} = f_{wd} \cdot l_w \cdot t_w \tag{7}$$

where  $f_{\rm wd}$  is the masonry failure stress, as obtained from diagonal compression tests on wallettes;

- (v) Lateral maximum strength (H<sub>max</sub> in Fig. 4), assumed equal to 1.3 times the cracking strength;
- (vi) Lateral residual strength ( $H_{res}$  in Fig. 4), taken equal to 5-10% of the peak strength.

Actually, there are multiple possible failure mechanisms for masonry infills, and for this reason the most correct approach is to calculate a strength value associated with each mechanism and adopt the lowest value when setting the strength of the equivalent diagonal strut. Decanini *et al.* [24] identify four different possible failure mechanisms: (a) compression at the centre of the panel, (b) compression of corners, (c) sliding shear failure and (d) diagonal tension. The equivalent compressive strength  $\sigma_{w,i}$  for each collapse mechanism is evaluated with the expressions reported in Table 6, where  $f_{sj}$  is the sliding resistance of the mortar joints,  $\sigma_v$  is the vertical compression stress due to gravity loads ,  $f_{wd}$  is the shear strength under diagonal compression and  $f_{wc}$  is the masonry compression strength. The peak strength of the equivalent strut is then calculated as:

$$N_{max} = \sigma_{w,min} \cdot t_w \cdot b_w \tag{8}$$

Table 6: Equivalent compressive strength corresponding to different collapse mechanisms of masonry infills.

$\sigma_{w,a} = \frac{1.16 f_{wc} \tan \theta}{\alpha_1 + \alpha_2 \lambda h}$	Diagonal compression failure
$\sigma_{w,b} = \frac{1.12 f_{wc} \sin \theta \cos \theta}{\alpha_1 (\lambda h)^{-0.12} + \alpha_2 (\lambda h)^{0.88}}$	Corner crushing
$\sigma_{w,c} = \frac{(1.2\sin\theta + 0.45\cos\theta)f_{sj} + 0.3\sigma_V}{b_w/d_w}$	Sliding of the bed joints
$\sigma_{w,d} = \frac{0.6f_{wd} + 0.3\sigma_V}{b_w/d_w}$	Diagonal tensile failure

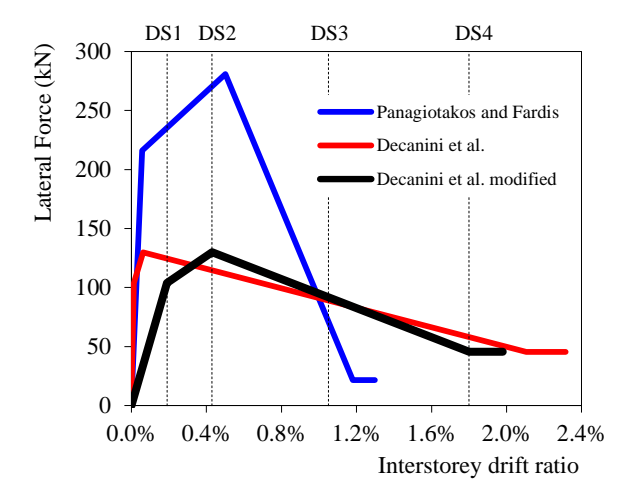
As in the model of Panagiotakos and Fardis [23], also the skeleton curve of the lateral force-displacement behaviour adopted in the model of Decanini *et al.* [24] presents four branches (see Fig. 4). The first linear elastic ascending branch corresponds to the un-cracked stage. The second branch refers to the post-cracking phase up to the attainment of the peak strength ( $H_{max}$ ), corresponding to extensive cracking of the infill panel. The descending third branch describes the post-peak strength degradation of the infill up to the attainment of a residual strength ( $H_{res}$ ).

In the model by Decanini *et al.* [24], the secant stiffness to peak strength ( $K_{sec}$  in Fig. 3), is evaluated computing the ratio  $b_w/d_w$  with the following expression:

$$\frac{b_w}{d_w} = \frac{\alpha_1}{\lambda h} + \alpha_2 \tag{9}$$

where  $\lambda h$  is calculated with Eq. (6) while  $\alpha_1$  and  $\alpha_2$  are coefficients that change according to  $\lambda h$  (Decanini *et al.* [24]). For instance, for  $\lambda h < \pi$ ,  $\alpha_1 = 1.3$  and  $\alpha_2 = -0.178$ .

The other parameters of the model by Decanini *et al.*[24] are derived from the following assumptions, supported by comparisons with experimental results (Parducci and Mezzi [26], Stylianidis [27]):  $K_1/K_{sec} = 4$ ,  $K_3/K_{sec} = 0.02$ ,  $H_{cr}/H_{max} = 0.8$ ,  $H_{res}/H_{max} = 0.35$ .



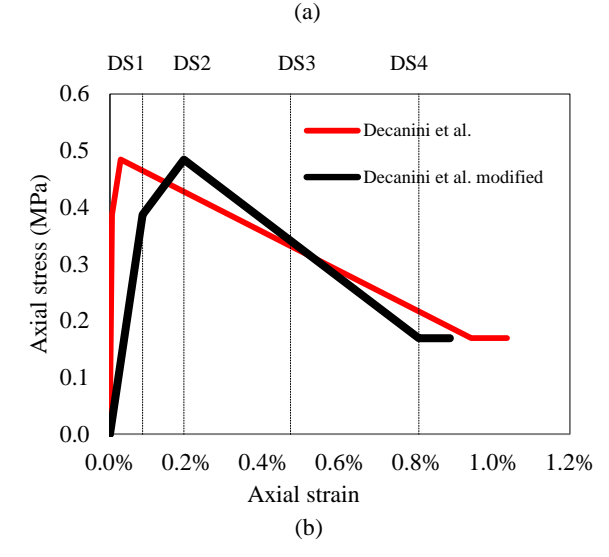


Figure 5: (a) Comparison between two well-known numerical models for masonry infills and the fragility function parameters derived in this study for different damage states of masonry infills, (b) impact of proposed modification to the Decanini et al. approach on the axial behaviour of the equivalent diagonal strut.

#### Use of Fragility Information to Characterize the Force-Displacement Curve of Masonry Infills

Figure 5 shows the lateral force vs. interstorey drift relationships derived from the models by Panagiotakos and Fardis [23] and Decanini *et al.* [24] for a typical masonry infill

panel, whose mechanical properties and geometric characteristics are reported in Tables 7 and 8, respectively. In Fig. 5 (a), the median values of the interstorey drifts associated with different DSs, derived in this study from regression of experimental results (see Table 4) are compared with the skeleton curves of the two selected numerical models. As can be seen, significant discrepancies are observed between numerical and experimental limit state drift values. In particular, both numerical models prematurely predict the onset of cracking (refer to DS1 in Fig. 5(a)). The model by Decanini et al. [24] moreover, largely underestimates the interstorey drift corresponding to the attainment of the peak strength (i.e. extensive cracking) of masonry infills (refer to DS2 in Fig. 5 (a)). On the other hand, the model by Panagiotakos and Fardis overestimates the degradation of the infill up to the attainment of the residual strength (refer to DS3 and DS4 in Fig. 5 (a)). The aforesaid discrepancies may result in poor estimation of engineering demand parameters (i.e. peak interstorey drifts and maximum floor accelerations) in nonlinear structural analysis and hence, inaccurate loss assessment in PBEE assessment.

As current modelling approaches for masonry infills appear to be based on a number of rough assumptions regarding stiffness ratios, a displacement-based modelling approach is proposed herein, which relies on the results (median values) of fragility curves to avoid arbitrary modelling assumptions, such as presumed stiffness ratios. In order to obtain better correlation between predicted and observed interstorey drifts associated with the different damage states of masonry infills, it is proposed that the axial stress vs. axial strain behaviour of the equivalent strut (see Fig.4 and Fig. 5 (b)) be set and modelled as follows: (i) the axial stress is derived from the force levels of the model of Decanini et al. [24], (ii) the axial strains are adjusted to fit the median values of axial strain derived from the literature review for the four selected damage states (Table 5). Table 9 compares the axial strains of the original and modified equivalent strut model for the case study under scrutiny.

This new modelling approach is considered advantageous because it provides a model that is calibrated to experimental results. Moreover, it provides consistency between the analysis and damage assessment phases within a performance-based engineering assessment; recognizing that masonry infill performance might be assessed either in a post-processing phase, using drift demands obtained from structural analyses together with fragility functions, or during the structural analysis phases, with direct modelling of the infills.

Table 7: Mechanical property	ies of weak and med	lium tung masangu can	sidered in this study
Tavie 7. Mechanicai properii	ies oj weak ana mea	лит-туре таѕоту соп	siaerea in inis siaay.

Brick unit	Mortar type	E <sub>m</sub> (MPa)	G <sub>m</sub> (MPa)	f <sub>wc</sub> (MPa)	f <sub>ws</sub> (MPa)	f <sub>sj</sub> (MPa)	σ <sub>w,a</sub> (MPa)	σ <sub>w,b</sub> (MPa)	σ <sub>w,c</sub> (MPa)	σ <sub>w,d</sub> (MPa)
Hollow masonry brick	Cement + sand	1458	583	1.2	0.4	0.3	0.91	0.68	0.61	0.48

Table 8: Geometric and mechanical characteristics of the examined infilled RC frame.

E <sub>c</sub> (MPa)	σ <sub>v</sub> (MPa)	h (m)	L (m)	t <sub>w</sub> (m)	h <sub>w</sub> (m)	L <sub>w</sub> (m)	θ (rad)	A <sub>c</sub> * (m <sup>2</sup> )	I <sub>c</sub> * (m <sup>2</sup> )	d <sub>w</sub> (m)	λh (m)
28960	0.00126	3.3	5.05	0.12	2.8	4.5	0.56	0.165	0.0042	5.30	1.95

<sup>\*</sup> RC columns with 550mm×300mm cross section

Table 9: Comparison between original and modified equivalent strut model.

		Medi	ium-type i	infill	
Model	drift N (kN)		ε	σ (MPa)	
Decanini et al. [24]	$\delta_{ m cr}$	122.30	0.06‰	0.39	
	$\delta_{max}$	152.88	0.28‰	0.48	
	$\delta_{res}$	53.51	9.42‰	0.17	
	$\delta_{\rm cr}$	122.30	0.85‰	0.39	
Decanini modified	$\delta_{max}$	152.88	1.93‰	0.48	
	$\delta_{res}$	53.51	8.06‰	0.17	

#### ESTIMATION OF LIKELY REPAIR COSTS

#### Introduction

As stated in the introduction, a modern performance-based earthquake engineering assessment may seek to quantify the repair costs expected following a certain intensity event. To assist with this, the repair costs associated with the various damage states described earlier (namely DS1, DS2, DS3 and DS4) are estimated in this section.

As explained earlier, the damage states considered in this work are distinguished on the basis of the description of physical damage in terms of cracking, crushing, etc. and the feasibility of repair. The lowest damage state (DS1) is assumed to correspond to the onset of cracking, requiring little more than cosmetic repairs. The second damage state (DS2) is associated with the removal of cracked and broken masonry units and their replacement, as well as the installation of any pipes or electrical wiring and replacement of ceramic tiles and other cosmetic repairs. The third damage state considered (DS3) provides a complete replacement of the wall, which includes removal of the old infill and the construction of a new wall. Possible additional costs to consider within this damage state include activities like the installation of eventual pipes or replacement of windows or doors within the infill. Finally, the fourth damage state (DS4) is also characterized by a demolition and consequent reconstruction of the infill wall but, in addition, requires the supply and installing of new windows/doors which, in DS3, are instead only removed and repositioned.

This paper presents cost estimates obtained two different ways; (i) using costing manuals (for Rome, Italy) and (ii) by obtaining quotes from the local construction industry in Rome, Italy.

### Repair Cost Estimates Obtained using Italian Costing Manuals

Tables 10-11-12-13 list the repair work envisaged for a given limit state, together with the cost of repair as obtained using the 2011 costing manual for the region of Rome, Italy. Note that the repair costs can be computed as a ratio of the replacement cost by dividing the total repair cost for each damage state by the DS3 repair cost.

Table 10: Damage State 1 repair cost estimates obtained using 2011 costing manuals (central Italy).

DAMAGE STATE	INTERVENTION	DESCRIPTION	ТҮРЕ	QNT	EURO	
	Scraping, finishing coat, pickaxing	Scraping for removal of old painting; finishing coat of old solid plaster; pickaxing of up 3 cm thick plaster, including brushing	Removal of lime, tempera and washable painting	Per m <sup>2</sup>	6.17	
	Background rendering new coat	Background rendering coat with cement mortar	Finishing coat with emulsion stucco	Per m <sup>2</sup>	25.51	
	Installation of a net for plaster	Net made by synthetic material for plaster reinforcement supplied and placed in work	Mechanical fastening to the wall substrate	Per m <sup>2</sup>	4.38	
DS1	Finishing new coat	Finishing coat of new plaster	Handmade	Per m <sup>2</sup>	5.28	
	Three coat plastering + Painting	Plaster formed by background rendering coat, floating coat and finishing coat; painting with washable paint of synthetic resin	Cement-lime mortar; internal surfaces with vinyl paints	Per m <sup>2</sup>	15.35	
			TOTAL	Per m <sup>2</sup>	56.69	
	ADDITIONAL FEATURES					
	Removal of tile coating	Carried out also with suitable tools, avoiding damage to the underlying masonry and to the systems	Ceramic tiles	Per m <sup>2</sup>	6.2	
			TOTAL	Per m <sup>2</sup>	62.89	

Table 11: Damage State 2 repair cost estimates obtained using 2011 costing manuals (central Italy).

DAMAGE STATE	INTERVENTION	DESCRIPTION	ТҮРЕ	QNT	EURO	
	Scraping, finishing coat, pickaxing	Scraping for removal of old painting; finishing coat of old solid plaster; pickaxing of up 3 cm thick plaster, including brushing	Removal of lime, tempera and washable painting	Per m <sup>2</sup>	6.17	
	Background rendering new coat	Background rendering coat with cement mortar	Finishing coat with emulsion stucco	Per m <sup>2</sup>	25.51	
	Installation of a net for plaster	Net made by synthetic material for plaster reinforcement supplied and placed in work	Mechanical fastening to the wall substrate	Per m <sup>2</sup>	4.38	
	Finishing new coat	Finishing coat of new plaster	Handmade	Per m <sup>2</sup>	5.28	
DS2	Three coat plastering + Painting	Plaster formed by background rendering coat, floating coat and finishing coat; painting with washable paint of synthetic resin	Cement-lime mortar; internal surfaces with vinyl paints	Per m <sup>2</sup>	15.35	
	Demolition of broken bricks	Demolition of building structures above ground level and at any height, including plasters and coatings	Evaluated for the effective cubic volume	Per m <sup>2</sup>	17.68	
	Masonry reconstruction	Masonry wall executed with bastard mortar; double wall with air chamber in between	Width between 30 to 40 cm	Per m <sup>2</sup>	61.86	
			TOTAL	Per m <sup>2</sup>	136.23	
	ADDITIONAL FEATURES					
	Removal of tile coating	Carried out also with suitable tools, avoiding damage to the underlying masonry and to the systems	Ceramic tiles	Per m <sup>2</sup>	6.20	
			TOTAL	Per m <sup>2</sup>	142.43	

Table 12: Damage State 3 repair cost estimates obtained using 2011 costing manuals (central Italy).

DAMAGE STATE	INTERVENTION	DESCRIPTION	ТҮРЕ	QNT	EURO	
	Demolition of the masonry infill wall	Demolition of building structures above ground level and at any height, including plasters and coatings	Evaluated for the effective cubic volume	Per m <sup>2</sup>	12.91	
	Masonry infill construction	Masonry wall executed with bastard mortar; double wall with air chamber in between	Width between 30 to 40 cm	Per m <sup>2</sup>	78.76	
	Thermal insulation	For internal walls	Preassembled	Per m <sup>2</sup>	34.6	
	Finishing new coat	Finishing coat of new plaster	Handmade	Per m <sup>2</sup>	5.28	
	Three coat plastering + Painting	Plaster formed by background rendering coat, floating coat and finishing coat; painting with washable paint of synthetic resin	Cement-lime mortar; internal surfaces with vinyl paints	Per m <sup>2</sup>	15.35	
			TOTAL	Per m <sup>2</sup>	146.90	
	ADDITIONAL FEATURES					
DS3	Ceramic tile coating	Supply and installation of interior wall coverings with ceramic tiles	Ceramic tiles	Per m <sup>2</sup>	29.11	
			TOTAL	Per m <sup>2</sup>	176.01	
	Pipes removal	Removal of iron pipes, gres, materials in polyvinyl or other plastic material inside the masonry	Pipes diameter from 60 mm to 110 mm	Per m <sup>2</sup>	12.42	
	Tracks for installations	Execution of tracks inside the infill	Infill thickness from 226 mm to 400 mm	Per m <sup>2</sup>	14.46	
			TOTAL	Per m <sup>2</sup>	204.930	
	Windows frame removal	Removal of interior or exterior opening frames	Disassembly of the fixed frame	Per m <sup>2</sup>	34.4	
	Windows frame repositioning	Reposition of the previously removed windows frame	Supply and installation	Per m <sup>2</sup>	57.12	
			TOTAL	Per m <sup>2</sup>	296.45	

Table 13: Damage State 4 repair cost estimates obtained using 2011 costing manuals (central Italy).

DAMAGE STATE	INTERVENTION	DESCRIPTION	ТҮРЕ	QNT	EURO	
	Demolition of the masonry infill wall	Demolition of building structures above ground level and at any height, including plasters and coatings	Evaluated for the effective cubic volume	Per m <sup>2</sup>	12.91	
	Masonry infill construction	Masonry wall executed with bastard mortar; double wall with air chamber in between	Width between 30 to 40 cm	Per m <sup>2</sup>	78.76	
	Thermal insulation	For internal walls	Preassembled	Per m <sup>2</sup>	34.6	
	Finishing new coat	Finishing coat of new plaster	Handmade	Per m <sup>2</sup>	5.28	
	Three coat plastering + Painting	Plaster formed by background rendering coat, floating coat and finishing coat; painting with washable paint of synthetic resin	Cement-lime mortar; internal surfaces with vinyl paints	Per m <sup>2</sup>	15.35	
			TOTAL	Per m <sup>2</sup>	146.90	
	ADDITIONAL FEATURES					
DS4	Ceramic tile coating	Supply and installation of interior wall coverings with ceramic tiles	Ceramic tiles	Per m <sup>2</sup>	29.11	
			TOTAL	Per m <sup>2</sup>	176.01	
	Pipes removal	Removal of iron pipes, gres, materials in polyvinyl or other plastic material inside the masonry	Pipes diameter from 60 mm to 110 mm	Per m <sup>2</sup>	12.42	
	Tracks for installations	Execution of tracks inside the infill	Infill thickness from 226 mm to 400 mm	Per m <sup>2</sup>	14.46	
			TOTAL	Per m <sup>2</sup>	204.93	
	Window removal	Removal of interior or exterior opening frames	Disassembly of the broken window	Per m <sup>2</sup>	34.4	
	New window installation	Supply and installation of simple window designed for the application of insulating glass with a single wood frame	Supply and installation	Per m <sup>2</sup>	237	
			TOTAL	Per m <sup>2</sup>	476.33	

Table 14: Repair costs quoted by building contractors in Rome for DS1 and DS3.

MANUFACTURERS	Euro/m² (DS1)	Euro/m² (DS3) without wiring	Euro/m² (DS3) with wiring
Building contractor n.1	100	153	803
Building contractor n.2	83	140	640
Building contractor n.3	44	73	373
Building contractor n.4	50	110	560
Building contractor n.5	89	173	673
Building contractor n.6	67	120	570
Building contractor n.7	56	100	500
Building contractor n.8	89	120	620
Building contractor n.9	100	133	733
Building contractor n.10	133	-	-
MEDIAN	81	125	608
DISPERSION	0.35	0.25	0.23

Nevertheless, the costing results obtained are considered quite useful for the whole of Italy, noting that even though construction costs outside of Rome will tend to reduce, the relative costs (i.e. the ratio of the DS1 to DS3 costs) are expected to be similar.

### **Indicative Repair Costs from the Italian Construction Industry**

In order to gauge the validity and dispersion expected for the cost estimates reported in the previous section, ten different building contractors in Rome were contacted and requested to provide cost estimates for the repair works described in the previous section. In all cases the contractors were not willing to provide a cost estimate for repair work associated with DS2 without first seeing the extent of the damage. Furthermore, one contractor would only provide repair cost estimates for DS1. Table 14 presents the results of this consultation process, reporting the repair costs quoted for damage states DS1 and DS3. The names of the building contractors are not reported for confidentiality reasons.

#### **Discussion of Cost Estimates Obtained**

Cost-estimates must always be treated with a degree of uncertainty. The results presented in the previous sub-sections have indicated, however, that masonry infill repair costs obtained from a costing manual do appear to reflect industry costs reasonably well, particularly for DS1, where the repair costs obtained using manuals came out at about 63 euro/m² whereas industry repair cost was 81 euro/m², but with several contractors quoting less than 60 euro/m². The replacement costs estimated by manuals for DS3 were higher than industry costs, possibly because the cost of undertaking the itemized list of activities separately will tend to cost more than if the

activities are done all together, as in the case of a masonry infill wall replacement.

Interpreting and using the results presented in the previous table should be done with care. No allowance was made for scaffolding costs, which should be included as a separate cost item, since scaffolding may also be required for external structural repairs and therefore is not specific to masonry infills. Furthermore, the cost estimates reported here do not allow for eventual reductions in unit repair costs that could be expected when large quantities of infill need to be repaired. Finally, the repair costs do not allow for the possibility of price-increases caused by an increase in demand on labour force following an earthquake event.

In addition to providing some information on the actual median costs of infill repair, note that the manufacturer survey has also provided some valuable insight into the possible variation (computed here as a value of dispersion and reported at the base of Table 14) in repair costs. This information, which is not usually provided in costing manuals, should be particularly useful for engineers wishing to make some account for uncertainty in infill repair costs as part of a refined performance-based loss estimation.

#### CONCLUSIONS

This work has focussed on characterizing the in-plane behaviour of masonry infills to better facilitate the performance-based earthquake engineering assessment of buildings possessing masonry infills. It is noted that despite numerous investigations into the behaviour of masonry infills in the past, there appears to be different proposals in the literature for the definition of damage states in infills. After choosing to adopt a visual definition of damage states, experimental data have been analysed in order to develop fragility functions for the in-plane deformation capacity. The results indicate that infill masonry can exhibit first signs of damage at drifts of less than 0.2% but may not suffer complete failure until drifts as high as 2.0%. Furthermore, it has been shown that masonry fragility changes significantly according to the type of infill masonry. Common infill modelling approaches have been briefly reviewed and it has been subsequently proposed that the deformation capacity of equivalent strut models could be set using the strain-based infill fragility information obtained in this work, rather than existing analytical expressions which do not appear to align well with experimental evidence. Finally, the work has revealed that there is reasonable correlation between Italian masonry infill repair cost estimates obtained using costingmanuals and those obtained through consultation with the industry, and some insight is provided into the likely dispersion in masonry infill repair costs. It is anticipated that the results of this work will be particularly useful for advanced performance-based earthquake engineering assessments of buildings with masonry infill, providing new information on the in-plane fragility, repair costs and non-linear modelling of masonry infills.

#### ACKNOWLEDGMENTS

The authors would like to acknowledge the funding provided by the 2014 and 2015 ReLUIS consortium in support of this work.

#### LIST OF SYMBOLS

EDP	<b>Engineering Demand Parameter</b>

 $F_i$ Conditional Probability

Φ Standard Normal cumulative distribution function

 $\overline{x}_{i}$ Median value of the probability distribution

 $\beta_i$ Logarithmic standard deviation

Frame centreline span L

h Centreline storey height

Strain capacity 3

θ Drift capacity

Initial (uncracked) shear stiffness  $K_1$ 

Lateral displacement of the storey  $d_{r}$ 

Masonry panel length  $l_{\rm w}$ Masonry panel thickness

 $t_{\rm w}$  $h_{\rm w}$ Masonry panel height

K<sub>sec</sub> Secant stiffness to peak strength

length of the equivalent strut  $d_{\mathbf{w}}$ 

Non-dimensional parameter depending on the λh geometric and mechanical characteristics

Young's modulus of masonry  $E_{m}$ 

Young's modulus of concrete  $E_{c}$ 

 $K_3$ Softening stiffness

Lateral cracking strength  $H_{cr}$ Masonry failure stress

 $f_{wd}$ Equivalent compressive strength

 $\sigma_{\rm w,i}$ Sliding resistance of the mortar joints  $f_{si}$ 

Vertical compression stress due to gravity loads  $\sigma_{v}$ 

 $f_{wd}$ Shear strength under diagonal compression

 $f_{wc}$ Masonry compression stress

Peak strength of the equivalent strut  $N_{max}$ 

#### REFERENCES

- New Zealand Standard (2004). "Structural Design Actions, Part 5: Earthquake Actions". NZS 1170.5:2004, Standards New Zealand, Wellington, NZ.
- New Zealand Standard (2006). "Concrete Structures Standards, Part 1: The design of concrete structures". NZS 3101:2006,, Standards New Zealand, Wellington, NZ.
- Ricci P, De LF and Verderame GM (2011). "6th April 2009 L'Aquila Earthquake, Italy: Reinforced Concrete Building Performance". Bulletin of Earthquake Engineering, 9(1): 285-305.
- Manzini CF and Morandi P (2012). "Rapporto preliminare sulle prestazioni ed i danneggiamenti agli edifici in muratura portante moderni a seguito degli delemiliani 2012". eventi sismici http://www.eqclearinghouse.org/2012-05-20, [in Italian].
- Yorulmaz M and Sozen MA (1968). "Behavior of Single-Story Reinforced Concrete Frames with Filler Walls". Technical Report to the Department of Defense No. 337, University of Illinois, Urbana.
- Angel R and Abrams D (2005). "Behavior of Reinforced Concrete Frames with Masonry Infills". Structural Research Series No. 589. Department of Civil Engineering, University of Illinois, Urbana-Champaign.
- Colangelo F (2005). "Pseudo-Dynamic Seismic Response of Reinforced Concrete Frames Infilled with Non-Structural Brick Masonry". Earthquake Engineering Structural Dynamic 2005, 34: 1219-1241.
- Morandi P, Hak S and Magenes G (2014). "In-plane Experimental Response of Strong Masonry Infills". 9th International Masonry Conference 2014, Guimaraes.
- Tasnimi AA and Mohebkhah A (2011). "Investigation on the Behaviour of Brick-Infilled Steel Frames with Openings: Experimental and Analytical Approaches". Engineering Structures, Elsevier, 33: 968-980.
- 10 Calvi GM and Bolognini D (2001). "Seismic Response of Reinforced Concrete Frames Infilled with Masonry Panels Weakly Reinforced". Journal of Earthquake Engineering, **5**(2): 153-185.

- 11 Kakaletsis DJ and Karayannis CG (2008). "Influence of Masonry Strength and openings on Infilled R/C Frames under Cycling Loading". *Journal of Earthquake Engineering*, DOI:10.1080, **12**(2): 197-221.
- 12 FEMA P-58 (2012). "Seismic Performance Assessment of Buildings: Vol. 1 Methodology". FEMA P-58-1, Prepared by the Applied Technology Council for the Federal Emergency Management Agency, Washington, D.C.
- 13 Porter KA (2003). "An Overview of PEER's Performance-Based Earthquake Engineering Methodology". Proceedings of Ninth International Conference on Applications of Probability and Statistics in Engineering, San Francisco, CA.
- 14 Meharbi AB and Shing PB (2003). "Seismic Analysis of Masonry-Infilled Reinforced Concrete Frames". TMS Journal, September 2003.
- 15 Hak S, Morandi P, Magenes G and Sullivan TJ (2012). "Damage Control for Clay Masonry Infills in the Design of RC Frame Structures". *Journal of Earthquake Engineering*, DOI: 10.1080, **16**(1): 35.
- 16 CEN (2004). "European Standard Eurocode 8: Design of Structures for Eathquake Resistance". EN 1998-1:2004, Comitè Européen de Normalisation, Bruxelles.
- 17 NTC (2008). "Norme Tecniche per le Costruzioni, decreto 14 febbraio 2008, G.U. 4 febbraio 2008 n. 29 S. O. n. 30". [in Italian].
- 18 FEMA E74 (2012). "Reducing the Risks of Nonstructural Earthquake Damages". Federal Emergency Management Agency, Practical Guide.
- 19 FEMA 273 (1997). "NEHRP Guidelines for the Seismic Rehabilitation of Buildings". Federal Emergency Management Agency, U.S. Department of Homeland Security, Washington DC, USA.
- 20 Porter K, Kennedy R and Bachman R (2007). "Creating Fragility Functions for Performance-Based Earthquake Engineering". *Earthquake Spectra*, **23**(2): 471-489.
- 21 Lilliefors HW (1967). "On the Kolmogorov-Smirnov Test for Normality with Mean and Variance Unknown". *Journal of American Statistical Association*, 62(318): 399-402.
- 22 Crisafulli FJ, Carr AJ and Park R (2000). "Analytical Modelling of Infilled Frame Structures - A General Review". Bulletin of the New Zealand Society for Earthquake Engineering, 33(1): 30-47.
- 23 Panagiotakos TB and Fardis MN (1994). "Proposed Nonlinear Strut Models for Infill Panels". 1st Year

- Progress Report of HCM-PREC8 Project, University of Patras.
- 24 Decanini L, Mollaioli F, Mura A and Saragoni R (2004). "Seismic Performance of Masonry Infilled RC Frames". 13th World Conference on Earthquake Engineering, No. 165, Vancouver, 2004.
- 25 Klingner RE and Bertero VV (1978). "Earthquake Resistance of Infilled Frames". *Journal of the Structural Division*, **104**(6): 973-989.
- 26 Parducci A and Mezzi M (1980). "Repeated Horizontal Displacements of Infilled Frames Having Different Stiffness and Connection Systems Experimental Analysis". Proceedings of The Seventh World Conference on Earthquake engineering, Istanbul, Turkey.
- 27 Stylianidis KC (1998). "Cyclic Behaviour of Infilled RC Frames". *Proceedings of 8th Conference IBMaC*. Dublin.
- 28 Schneider SP and Abrams DP (1998). "Lateral Strength of Steel Frames with Masonry Infills Having Large Openings". *Journal of Structural Engineering*, **124**: 896-904.
- 29 Sigmund V and Penava D (2012). "Experimental Study of Masonry Infilled R/C Frames with Openings". 15<sup>th</sup> World Conference on Earthquake Engineering, Lisbon, 2012.
- 30 Mosalam KM, White RN and Gergely P (1997). "Static Response of Infilled Frames Using Quasi-Static Experimentation". *Journal of Structural Engineering*, **123**: 1462-4169.
- 31 Guidi G, da-Porto F, Dalla-Benetta M, Verlato N and Modena C (2013). "Comportamento Sperimentale nel Piano e Fuori Piano di Tamponamenti in Muratura Armata e Rinforzata". Dipartimento di Ingegneria Civile, Edile e Ambientale, Padova, [in Italian].
- 32 Pujol S, Benavent-Climent A, Rodriguez ME and Smith-Pardo P (2008). "Masonry Infill Walls: an Effective Alternative for Seismic Strengthening of Low-Rise Reinforced Concrete Building Structures". 14<sup>th</sup> World Conference on Earthquake Engineering, Beijing, China.
- 33 Hashemi A and Mosalam KM (2007). "Seismic Evaluation of Reinforced Concrete Buildings Including Effects of Masonry Infill Walls". PEER Report 2007/100, University of California, Berkeley.
- 34 Colangelo F, Biondi S and Nuti C (1997). "Prove pseudo-dinamiche su telai tamponati progettati secondo le norme italiane e l'Eurocodice n° 8". Atti, 8° Convegno Nazionale L'Ingegneria Sismica in Italia, Taormina, 2: 987-994, [in Italian].